

Synchronous PM Machine Design, Analysis and Parameter Optimization

Arif Emre Yıldız
Electrical-Electronics Engineering
Abdullah Gul University
Kayseri, Turkey
arifemre.yildiz@agu.edu.tr

Samet Yılmaz
Electrical-Electronics Engineering
Abdullah Gul University
Kayseri, Turkey
samet.yilmaz@agu.edu.tr

Ömer Faruk Karadağ
Electrical-Electronics Engineering
Abdullah Gul University
Kayseri, Turkey
omerfaruk.karadag@agu.edu.tr

Abstract—The aim of this project is to design, analyse, and optimize a synchronous permanent magnet (PM) machine. The task's precise needs include an 8 pole, 36 slot, 7000 W motor running at 2000 rpm. The primary goal is to maximize the motor's efficiency while lowering its cost by reducing total mass. The optimization technique considers elements such as terminal voltage peak and torque ripple. For advanced simulations and analysis, ANSYS Maxwell is used. This project seeks to produce a high-performance synchronous PM machine that meets efficiency criteria while optimizing cost by thoroughly studying numerous characteristics and design elements.

Keywords— Synchronous PM Machine, ANSYS Electronics, Motor Design and Optimization, Finite Element Analysis (FEA)

I. INTRODUCTION

High-performance electrical machine design and analysis are critical for attaining efficient energy conversion between electrical and mechanical power. Synchronous Permanent Magnet (PM) machines have emerged as key options in applications requiring precise and constant speed control. Due to their ability to produce high output power performance and efficiency, these machines are widely used in a variety of equipment such as robot actuators, ball mills, clocks, record players, and turntables [1].

The purpose of this research is to develop, analyse, and optimize an 8-pole, 7000 W, 2000 rpm synchronous permanent magnet (PM) machine. Neodymium Iron Boron (NdFeB) magnets were chosen for this design because to their high remanent flux density and coercivity, ensuring the development of a durable motor with low demagnetization risk. Because these motors are vital and widely utilized, it is critical that the appropriate precautions be taken to produce the desired torque and voltage results.

Another goal of this study is to increase the performance of the synchronous PM machine using modern technical techniques and simulations. Comprehensive analysis and simulations will be performed using ANSYS software to fine-tune the motor settings, resulting in optimal efficiency while also decreasing total magnet volume and torque ripple. By completing this project, it is hoped to contribute to the field of electrical machinery design and support the development of high-performance, energy-efficient systems.

II. RELATED WORK

Synchronous permanent magnet (PM) machines have received a lot of attention in recent years because of their excellent performance qualities, such as high efficiency, compact size, and accurate speed control capabilities. When compared to other types of electrical machines, these

machines use permanent magnets on the rotor to generate a magnetic field, resulting in higher performance and lower energy loss [2]. Large research and development efforts have been dedicated toward the design, analysis, and optimization of synchronous PM machines due to the rising demand for energy-efficient systems.

A. Considerations for Design and Optimization Techniques

To ensure optimal performance, the design of synchronous permanent magnet (PM) devices must take into account a number of criteria. The number of poles, output power, operating speed, voltage, and current ratings, among other design parameters, have a considerable impact on the machine's efficiency and overall cost [3]. It is critical to balance these design elements in order to get the necessary performance characteristics.

In the design of synchronous PM machines, researchers have frequently used optimization approaches to enhance efficiency, reduce costs, and meet specific objectives. To achieve these objectives, multi-objective optimization, adaptive objective optimization, and mixed-integer sequential quadratic optimization methods have been widely used.

B. Trade-offs and Performance Metrics

For synchronous permanent magnet (PM) machines, efficiency is a critical performance metric. Higher efficiency means less energy consumed and better overall system performance. To achieve high efficiency, losses must be minimized, magnetic circuit design must be optimized, and torque ripple must be reduced [4]. Furthermore, because they affect the machine's overall performance and stability, terminal voltage peak value and torque ripple are key considerations in the optimization process. To achieve the appropriate balance, trade-offs between various performance measures must be carefully examined.

C. Applications of Synchronous PM Machines

Synchronous permanent magnet (PM) machines are becoming increasingly used in a wide range of industries, including robotics, renewable energy systems and electric vehicles. They are well-suited for these demanding applications due to their great efficiency, compact size, and accurate speed control capabilities.

Synchronous PM machines are utilized as actuators in the robotics sector to obtain precise motion control [5]. This is critical for robots that must move rapidly and precisely, such as those used in surgery or manufacturing.

In renewable energy systems, synchronous PM machines are used in wind turbines and hydroelectric generators to efficiently convert mechanical energy into

electrical energy. [6]. This is critical in order to meet the growing demand for renewable energy sources.

The low size and high-power density of synchronous PM machines help electric vehicles. This enables electric vehicles to have a longer range and better performance [7].

Synchronous PM machines are a versatile and powerful technology with numerous applications. They are well-suited for demanding applications in a range of industries due to their high efficiency, compact size, and accurate speed control capabilities.

III. METHOD

A. Modelling and parametrization

As referred, the goal is to design an optimum 8 pole 7000W synchronous PM machine. To achieve this goal, a PM machine that has 36 slots is drawn in ANSYS Maxwell 2D. In the design, the stator outer diameter was chosen as 340 mm. Other variables were parametrized, and the materials were assigned. For the stator and rotor material M19 29G steel is chosen as best material because of its high saturation point in B-H curve and having high permeability. Furthermore, the steel reduces the effects of eddy current and has the ability of operating in high temperatures. As the permanent magnet material, NDF 35 is chosen in ANSYS library. Finally, the motor is modelled as in the figure 1.

Modelling the motor is followed by the deriving several formulas to understand the features of the motor. One of the important formulas is the calculation of the resistance of the copper wires wrapped in slots of the motor. For this calculation, firstly, the length of the single turn of copper is required to be calculated. The single turn copper length ($L_{total/turn}$) can be calculated as rectangular, as it showed in the Fig. 3. Two side of the rectangle is the depth of the motor (L_{depth}) and other 2 side is an arc of the circle of the motor as it showed in figure 2. The arc length (L_{arc}) is calculated by using the number of slots that motor has which is 36 and the number of slots that the arc scans which is 5. Because the arc length is calculated, the radius from the center to mid-point of the slot is important. By using these parameters, the arc length can be calculated (1). The formula is approximated by increasing its value. The reason behind this approximation is that the copper wires will be curved a bit from the motor which means the length will be a bit longer than the calculation. The L_{arc} is found as 139.6mm. As it is indicated above, the length of wire for single turn can be calculated as multiplying the arc length and motor depth length by 2 (2).

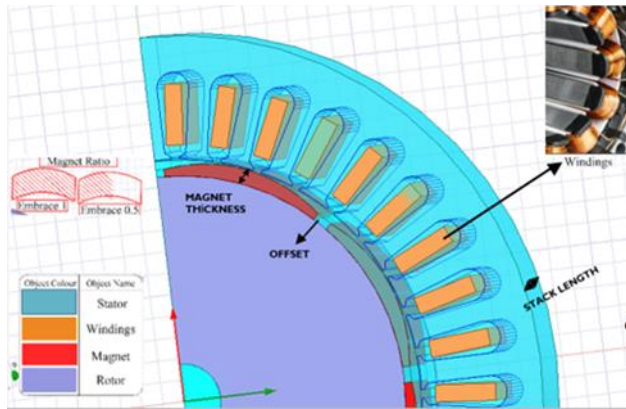


Figure 1. Design Geometry of PMSM

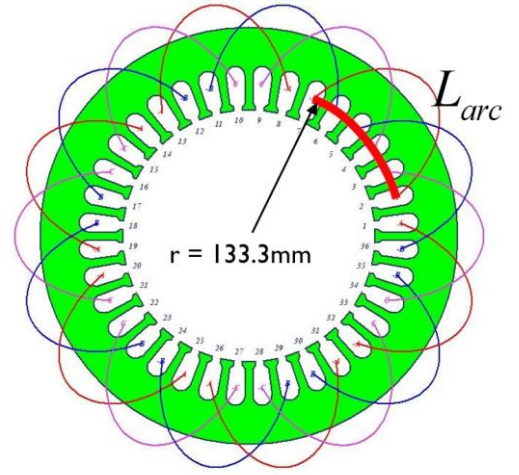


Figure 2. Arc length calculation for copper length

From the relevant equation the $L_{total/turn}$ was found as 355.18mm. Because there is N_t turns in one winding and 6 winding in single phase, the wire length of single phase ($L_{total/phase}$) can be calculated by multiplying the single turn length with the $6 \cdot N_t$ (3). The $L_{total/phase}$ is resulted as 25.57m.

$$L_{arc} = 2\pi r \cdot \frac{5}{36} = \frac{5\pi r}{18} \rightarrow \text{approximated as } \frac{6\pi r}{18} = \frac{\pi r}{3} \quad (1)$$

$$L_{total/turn} = 2L_{arc} + 2L_{depth} \quad (2)$$

$$L_{total/phase} = L_{total/turn} \cdot N_t \cdot 6 \quad (3)$$

By derived formulas of the copper length, the resistance of the copper per phase (R_{phase}) can be calculated. The formula of the copper resistance uses copper resistivity (ρ), length and cross-sectional area (4). In the formula, the area of the copper (A_c) can be found as multiplication of slot area (A_{slot}) and fill factor divided by number of turns (N_t) (5). The area of the slot can be driven from ANSYS design. By inserting the variables of resistivity is $1.72 \cdot 10^{-8} \Omega m$, length=25.57m, fill factor is 0.4, Number of turn per slot is 12, and cross-sectional area is $16mm^2$, the resistance value is found as $27m\Omega$. From the copper cross-sectional area, the radius of the copper is found as 2.25mm (6), and AWG is determined as 5AWG by looking at the wire gauge table.

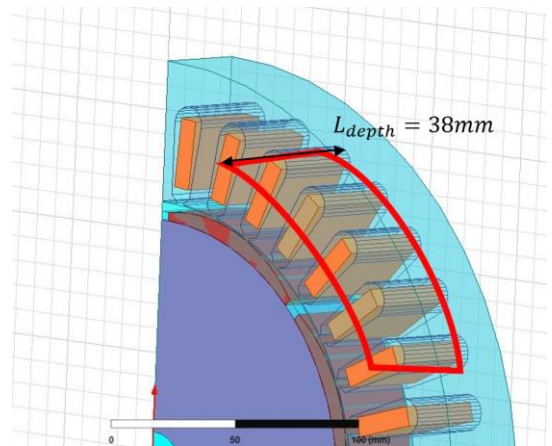


Figure 3. Winding Rectangular Representation for Copper Length

To check if there is an abnormal situation on the copper, caused by current amount, the current density can be calculated. The general formula for the current density is the current divided by copper area (7). The current value (I_{peak}) can be got from ANSYS simulation results and to find its rms value, the current is divided by square root of 2. In the denominator, (5) can be used as the cross-sectional area of the copper. The result of the current density formula is 2.047 A/mm^2 .

$$R_{phase} = \frac{\rho \cdot l}{A} = \frac{\rho \cdot L_{total / phase}}{A_c} \quad (4)$$

$$A_c = \frac{A_{slot} \cdot fill\ factor}{N_t} \quad (5)$$

$$\pi r^2 = A_c \rightarrow r = \sqrt{\frac{A_c}{\pi}} \quad (6)$$

$$CurrentDensity = \frac{I}{A_c} = \frac{I_{peak} / \sqrt{2}}{\frac{A_{slot} \cdot fill\ factor}{N_t}} = \frac{N_t \cdot I_{peak}}{A_{slot} \cdot fill\ factor} \quad (7)$$

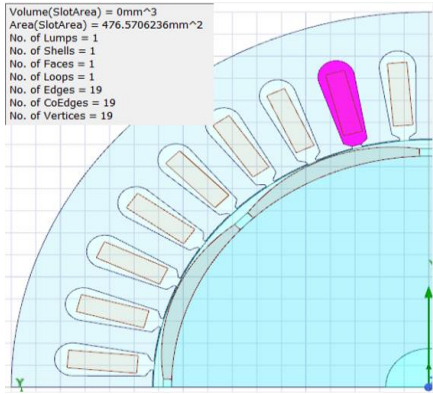


Figure 4. Slot Area Representation

In the motor, the conversion of frequency to rotational speed and vice versa. The frequency (f) can be found as the multiplication of rotational speed (n_s) and pole number (p) divided by 120 (8). Base speed of the designed motor is 2000rpm and it has 8 poles which means the f is 133.3Hz.

$$f = n_s \cdot \frac{p}{120} \quad (8)$$

B. Efficiency and cost analysis

The efficiency is a crucial when measuring how conversion of electrical power is converted to electrical power effectively. Basically, the efficiency in percentage is calculated by output power (P_{out}) divided by input power (P_{input}) and multiplied with 100 (9). In this project only the copper losses have considered. That is why the expected efficiency is high. The input Power is driven by summation of output power and the copper loss (P_{cu}). The copper loss is calculated by the phase current (I_{phase}) times the phase resistance of the copper (R_{phase}). Due to having 3 phases, the loss is multiplied with 3 to obtain the total loss (10). In the numerator of the efficiency formula, the output power

is related with torque (T) and rotational speed (n_s). Multiplication of them gives the output power (11). Through these formulas the output power came out as 7.04kW and the copper losses as 87W. That is why the efficiency is 98.78% as it is expected.

$$Efficiency = \frac{P_{out}}{P_{input}} \cdot 100 = \frac{P_{out}}{P_{out} + P_{cu}} \cdot 100 \quad (9)$$

$$P_{cu} = 3 \cdot I_{phase}^2 \cdot R_{phase} \quad (10)$$

$$P_{out} = T \cdot n_s \quad (11)$$

Apart from the efficiency, minimization of motor cost is another essential goal. The cost of the PM motor is related to how much material is used. These materials are core material and permanent magnets. In the mass calculation of the permanent magnet (M_{PM}), the area of single magnet (A_{PM}), motor length (L_{motor}), and its density (d_{magnet}) were multiplied. There are 8 poles in the system. Therefore, the magnet mass is also multiplied with the 8 (12). From this equality the mass of the magnets is totally calculated as 1kg. As in the magnet mass calculation, the mass of the rotor and stator (in total M_{steel}) are calculated as 19.07kg by multiplication of area, motor length, and density (13).

$$M_{PM} = A_{PM} \cdot L_{motor} \cdot d_{magnet} \cdot pole\ number \quad (12)$$

$$M_{steel} = (A_{stator} + A_{rotor}) \cdot L_{motor} \cdot d_{steel} \quad (13)$$

C. Voltage and Torque Calculations

On of the parameters that is considered and tried to be kept under 100V is peak value of phase voltage. Dividing the maximum voltage value of the phase voltage to $\sqrt{2}$, gives the phase voltage in RMS. The phase voltage (V_{phase}) can be approximated as summation of the induced back emf voltage (E_b) and voltage on the copper resistance (14). The voltage on the copper resistance is directly calculated via ohm's law. From the analysis of the design, the maximum phase voltage value is measured as 97.65V.

$$V_{phase} = E_b + I_{phase} \cdot R_{phase} \quad (14)$$

Another parameter that is maximum torque ripple that is limited to 30% to prevent vibrations and noises. Minimization of torque ripple will contribute to the power consumption and reduce it. To analyse the maximum torque ripple (ΔT) in the simulation, the peak-to-peak value of torque (T_{pp}) is divided by the average torque (T_{avg}). The result is multiplied with 100 for finding it in percentage. The maximum torque ripple is calculated as 2.22% which is very below the 30% limitation. It would be concluded that the designed motor didn't have vibrational problem and its power consumption is reduced fortunately.

$$\Delta T = \frac{T_{pp}}{T_{avg}} \cdot 100 \quad (15)$$

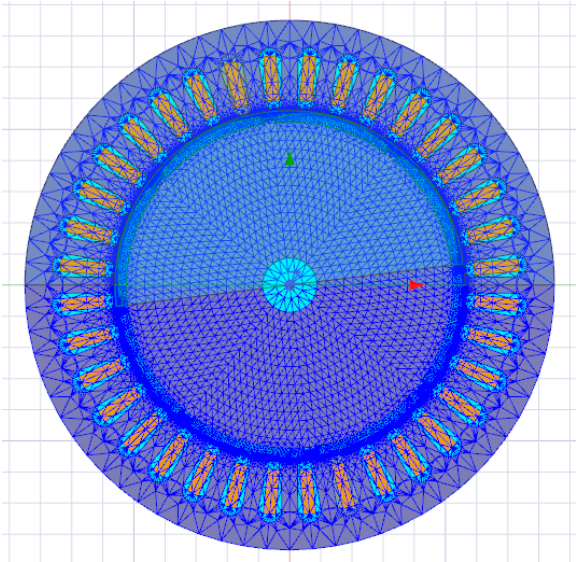


Figure 5. Mesh plot of the PMSM

D. Mesh setting of the motor

Mesh is a network structure that divides a model's geometry into small elements and uses these elements to perform calculations for simulation. Mesh refinement refers to determining the parameters used to divide the model's geometry into elements. These parameters include element size, element count, and element type, among others. Mesh refinement affects the accuracy of the simulation, computation time, and resource usage. Therefore, a good mesh refinement captures sufficient detail to obtain accurate results, optimizes computation time, and manages resource usage. As seen in Figure 5, detailed meshing is applied particularly to the air gap, magnet, and rotor surface sections of the motor.

IV. EFFECT OF PARAMETERS ON MOTOR PERFORMANCE

The effects of the parameters used in the motor to the motor have been observed and the effects of the parameters on the output results can be seen in Table I.

TABLE I. EFFECT OF INPUT PARAMETERS ON OUTPUTS

Parameters	↑↓	Torque	Torque Ripple	Output Power	Induced Voltages	Mass
Magnet Thickness	↓	↓	↓	↓	↓	↓
Offset	↓	↑	↑	↑	↑	↑
Embrace	↓	↓	↑	↓	↓	↓
Stack Length	↑	↑	↔	↑	↑	↑
Number of Turn	↑	↑	↑	↑	↑	↑
Airgap	↑	↓	↓	↓	↓	↑
Current	↓	↓	↓	↓	↓	↔

When looking at this Table I, it is deemed necessary to explain the influence of certain parameters on the motor's outputs. The considerations in this Table I are valid for the limits shown in Table II. Values outside these limits were not observed. Firstly, reducing the magnet thickness results in a decrease in the motor's mass due to the reduction in magnet mass. Decreasing the offset value primarily leads to a reduction in torque ripple. Similarly, reducing the offset value causes a decrease in magnet mass as it reduces the volume of the magnet. Looking at the embrace value, a decrease in this value results in a reduction in mass due to changes in the arc length of the magnets while increasing

torque ripple. These changes are more pronounced for a magnet with an offset. The stack length value represents the thickness of the motor and is directly related to efficiency and torque, being proportional to them. Therefore, increasing the stack length enhances efficiency, motor torque, and generated output power, but it also comes with a cost. The motor's mass increases, and losses within the motor may increase. Hence, it is necessary to perform a cost analysis and find optimal values considering that every increase or decrease has a cost associated with it. This is why the need for optimization arises. When examining the number of turns, it is observed that it is directly proportional to torque, torque ripple, output power, and induced voltage. However, increasing the number of turns means increasing the amount of copper used, resulting in an increase in copper loss within the motor. Similarly, an increase in copper mass occurs due to the increased amount of copper used, leading to an increase in the motor's mass.

Another significant parameter is the air gap value. Increasing the air gap between the rotor and stator generally affects the motor's mass. However, this effect can vary depending on the magnitude of the air gap increase and other design parameters and components of the motor. As the air gap increases, the gap between the rotor and stator widens, naturally increasing the overall volume and thus the mass of the motor. Unless other design parameters such as rotor and stator material thickness change, a wider air gap generally results in a larger motor mass. However, the effect of air gap increase on the motor's mass is usually small and balanced with other design factors. Increasing the air gap allows for more efficient passage of the magnetic field, which can affect motor performance. This may imply that the motor can have a higher capacity for generating torque. The last parameter, current value, is directly proportional to torque. Up to a certain threshold, doubling the current can lead to a proportional increase in torque. In addition, the current is directly proportional to the output results. Increasing the current not only increases torque but also increases output power. Optimization studies have been conducted to ensure that these values fall within the desired ranges and optimal conditions.

V. OPTIMIZATION

Two distinct types of optimization techniques, namely Multi-Objective Genetic Algorithm (Random Search) and Adaptive Multiple Objective Random Search, are employed to optimize the performance of the PM machine. The primary objective of this optimization process is to generate desired power output and torque values for the Permanent Magnet Synchronous Machine (PMSM). The input current and voltage are utilized to calculate the input power, while it is crucial to minimize copper loss, as it can lead to a decrease in efficiency by reducing the power output and torque.

During the setup phase of optimization, logical design parameters are established by considering the initial design that meets the desired outcomes. ANSYS Electromagnetics, a software system, necessitates a range of variables and objectives to apply its algorithm for system optimization. The specific objectives for this optimization process are outlined in Table II. These objectives are

utilized in conjunction with multi-objective genetic algorithms.

The size of the stator and rotor are fixed. The dimensions of the stator and rotor remain untouched in the optimization. Slot parameters and parameters such as Hs1, Bs1, and Hs2 that make up the slot were also not used in the optimization. On the other hand, the parameters affecting the main outputs of the motor are given in table II. Expectations from the optimization result can be seen in table III.

TABLE II. DESIGN PARAMETER

Parameter of Design	Constraints of Parameters
Airgap (Ag)	0.25 - 1
Embrace	0.75 - 0.95
Offset	0 - 45 (mm)
Number of turns per slot	3 - 50
Ipeak (Current)	3 - 50 (A)
Magnet Thickness	4 - 9 (mm)
Stack Length	20 - 60 (mm)

While determining the limits of the parameters given to the optimization, geometrically consistent limits were chosen. Most of these limits have been found by experimenting with motor simulation in ANSYS electronics.

TABLE III. DESIGN PARAMETER GOALS

Output Parameters	Goals	Optimization Weight
Efficiency	> 94	[1]
Total Mass	<25	[1]
Torque	>32.5	[1]
Output Power	=7000	[1]
Terminal Voltage	<100	[1]
Torque Ripple	<30	[1]

In this project, the key requirements for designing a synchronous permanent magnet (PM) machine were identified as follows: an output power of 7000W, a maximum terminal voltage of 100V, and a base speed of 2000 rpm. The project objective was to achieve three primary goals: maximize efficiency, minimize the total mass of the PMs to reduce costs, and limit torque ripple to a maximum of 30%. The optimization process was conducted with the objective of achieving the optimal cost value that minimizes the error in reaching the desired parameters. The resulting cost graph, depicted in Figure 6, illustrates the progression of cost values during the optimization process.

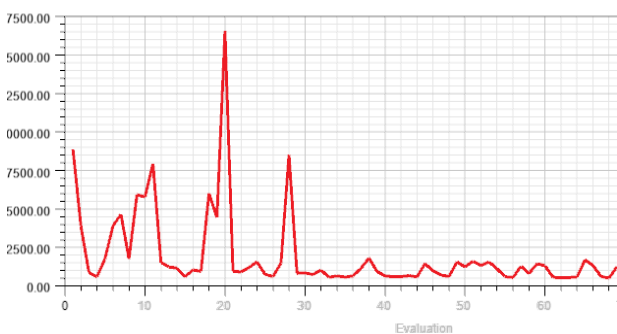


Figure 6. Graphical Representation of Cost Optimization Using a Multi-Objective Genetic Algorithm.

As seen in Figure 7, according to the optimization results, the motor was started by applying the minimum cost parameters and the output parameters were checked. Later, the optimized motor was obtained.

Variation	Airgap	Embrace	FillFactor	Hs0	Hs1	Ipeak	Ki	Ks	Le1	MagThick	MotorLength	R1	Rs	Sto	Tw	conds
1	0.252	0.751	0.4	0.7	1.2	3.235A	0	0	8.6	4.03mm	25.275mm	0	0	28	0	5.475
2	0.257	0.851	0.4	0.7	1.2	18.90	0	0	8.6	4.575454	29.505769mm	0	0	28	0	10.475
3	0.262	0.801	0.4	0.7	1.2	34.56	0	0	8.6	5.120909	33.736538mm	0	0	28	1	15.475
4	0.267	0.901	0.4	0.7	1.2	8.457	0	0	8.6	5.666363	37.967308mm	0	0	28	1	20.475
5	0.272	0.776	0.4	0.7	1.2	24.12	0	0	8.6	6.211818	42.198077mm	0	0	28	1	25.475
6	0.277	0.876	0.4	0.7	1.2	39.79	0	0	8.6	6.757272	46.428846mm	0	0	28	2	30.475
7	0.282	0.826	0.4	0.7	1.2	13.67	0	0	8.6	7.302727	50.659615mm	0	0	28	2	35.475
8	0.287	0.926	0.4	0.7	1.2	29.34	0	0	8.6	7.848181	54.890385mm	0	0	28	2	40.475
9	0.292	0.7635	0.4	0.7	1.2	45.01	0	0	8.6	8.393636	59.121154mm	0	0	28	3	45.475
10	0.297	0.8635	0.4	0.7	1.2	4.975	0	0	8.6	8.939090	63.351923mm	0	0	28	3	50.475
11	0.302	0.8135	0.4	0.7	1.2	20.64	0	0	8.6	9.484545	67.582692mm	0	0	28	3	55.475
12	0.307	0.9135	0.4	0.7	1.2	36.30	0	0	8.6	4.079586	71.813462mm	0	0	28	4	60.475
13	0.312	0.7885	0.4	0.7	1.2	10.19	0	0	8.6	4.625041	76.044231mm	0	0	28	4	65.475
14	0.317	0.8885	0.4	0.7	1.2	25.86	0	0	8.6	5.170495	25.800444mm	0	0	28	4	70.475
15	0.322	0.8385	0.4	0.7	1.2	41.53	0	0	8.6	5.715950	29.831213mm	0	0	28	5	75.475

Figure 7. Optimization Results for different variation

As seen in Table III, the control of the targeted output parameters was checked by looking at the optimized motor geometry and the motor took its final form.

VI. RESULTS AND DISCUSSION

The optimization outcomes are categorized into five sub-topics, which include examining the impact of parameters on power output, induced voltages, torque, saturation checkpoints (Magnetic Flux Density, Vector Fields), efficiency results, and efficiency mapping in relation to varying loading current and motor speed. The optimization process focuses on achieving the rated power by modifying certain motor parameters such as stack length, magnet thickness, air gap. Moreover, utilizing “Optimetrics” within ANSYS, the optimization procedure was executed to determine the optimal motor design among numerous candidates, with mass and efficiency as the primary criteria. A representative outcome of this optimization process is showcased in Figure 8.

Load Condition	I Peak (A)	Speed (rpm)	Average Torque (N.m)	Efficiency	Output Power (kw)	Torque Ripple
25%	11.5A	500	8.446	98.77%	0.442	1.81%
	11.5A	1000	8.4479	99.38%	0.884	
	11.5A	1500	8.448	99.56%	1.32	
	11.5A	2000	8.449	99.69%	1.77	
50%	23A	500	16.87	97.57%	0.883	1.84%
	23A	1000	16.871	98.75%	1.76	
	23A	1500	16.879	99.17%	2.65	
	23A	2000	16.88	99.38%	3.53	
75%	34.5A	500	25.277	96.39%	1.32	1.97%
	34.5A	1000	25.2774	98.16%	2.64	
	34.5A	1500	25.2775	98.77%	3.97	
	34.5A	2000	25.2775	99.074%	5.294	
100%	46A	500	33.614	95.24%	1.76	2.22%
	46A	1000	33.616	97.56%	3.52	
	46A	1500	33.6167	98.36%	5.28	
	46A	2000	33.6167	98.76%	7.04	

Figure 8. Output results for 16 different cases

The chosen design exhibits a combined mass of 19.32 kg for magnet and steel mass, while achieving an efficiency of 95.039% under rated load conditions.

The results obtained at different load conditions and speed values of the motor are presented in the figure 7. When the results are examined, it is seen that the motor achieves high efficiency at low current values. For example, while the efficiency of the motor is 98.77% at 11.5A current, at 500 rpm, the efficiency is 97.57% at the same speed at 23A current. In addition, it is observed that the efficiency values of the motor increase at high speeds (2000 rpm). While the efficiency of the motor was 99.69% at a current of 11.5A at 2000 rpm, the efficiency was measured as 99.38% at the same speed at a current of 23A. The output power of the motor is also calculated and added to the figure 8. Considering the efficiency values and torque values obtained, it is seen that the motor produces lower torque at low speeds and higher torque at high speeds at 11.5A current, but there are very small differences between these torque values, that is, there is no noticeable change in torque values.

TABLE IV. FINAL PARAMETER RESULTS

Parameter	Final Value
Airgap (Ag)	0.75
Embrace	0.91
Offset	38 (mm)
Number of turns per slot	12
Ipeak (Current)	46 (A)
Magnet Thickness	6.7 (mm)
Stack Length	38 (mm)

Various attempts were made to optimize the motor parameters and the most suitable values were determined. Below is the information of the parameters and values selected as a result of the optimization:

Airgap (Ag): In PMSM motors, the space between the rotor and the stator is called the air gap. This gap ensures the interaction of the magnet and the winding. Airgap refers to the distance between the rotor and the stator and has a significant effect on the efficiency of the magnetic circuit. The optimum airgap value is carefully chosen to maximize magnetic flux, reduce magnetic losses and optimize motor performance.

Offset: Offset refers to the geometrical harmony of the rotor magnet with the stator in the magnetic circuit. The offset value determines the position of the magnet and the air gap between the rotor and the stator. Choosing a correct offset value optimizes the magnetic flux, reduces magnetic losses, and increases the efficiency of the motor. The offset value is related to the geometry of the magnet and the rotor-stator configuration. Increasing the offset reduces the ripple in torque.

Number of turns per slot: This value refers to the number of winding wires in each slot of the stator. The number of turns per slot plays an important role in the design and performance of the winding. A higher number of turns can increase the torque output of the motor but can also affect winding resistance and copper losses.

Magnet Thickness: Magnetic material thickness was chosen as 6.7 mm. This value has been determined to increase the magnetic flux density and optimize the performance of the motor.

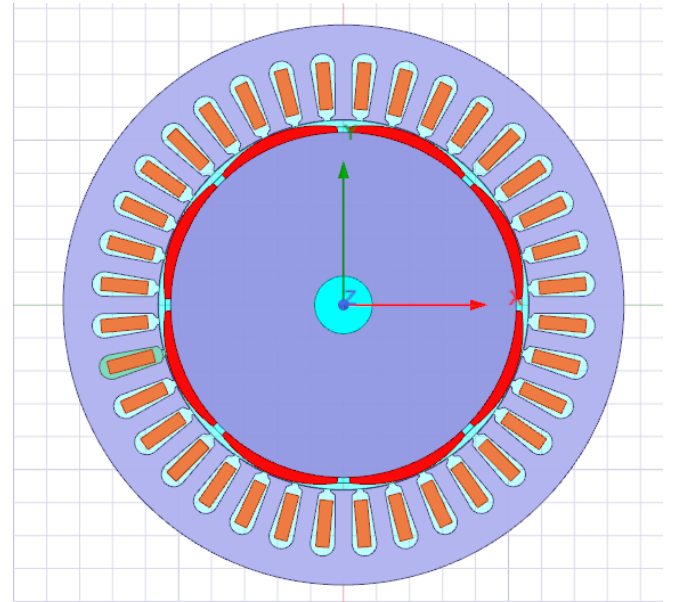


Figure 9. Optimized final motor design

The magnetic flux lines graph in figure 10, illustrates the distribution of the magnetic field of the PMSM motor. This graph shows how the magnetic flux moves between the rotor and stator.

Magnetic flux lines represent the direction and intensity of the magnetic field. The values of 0.0272 A/Wb and -0.0272 A/Wb in the graph show the intensity of the magnetic flux. Positive and negative values indicate that the magnetic flux is moving in different directions.

Since it is a motor with 8 poles, 8 poles can be observed in the graph. Poles are points where magnetic flux concentrates and creates a magnetic connection between rotor and stator. The number of poles determines the magnetic structure of the motor and how the magnetic flux is distributed. Moreover, the graph of magnetic flux lines is important to understand how the magnetic flux moves in the motor. When the graph is examined carefully, it can be observed how the magnetic flux circulates between the rotor and the stator and the regions where the magnetic field is intense.

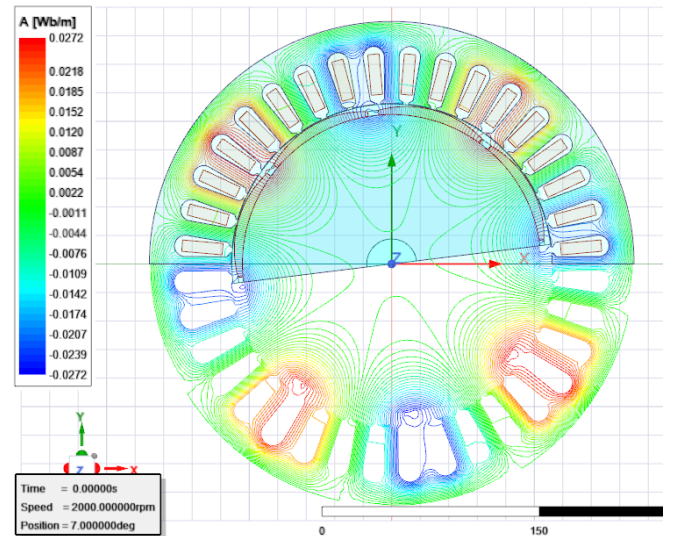


Figure 10. Magnetic Flux Lines Graph

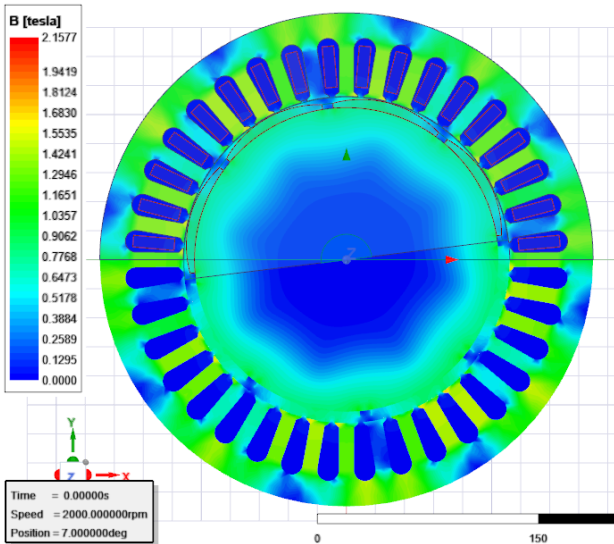


Figure 11. Magnetic Flux density Graph

The Magnetic Flux Density graph represents the distribution of magnetic flux density in a PMSM motor. The values in this graph represent the intensity of the magnetic field. The highest value observed is 2.15 Tesla. The stator is generally depicted in green, and the magnetic field intensity in this region is 1.2 Tesla. The values between two slots range from 1.42 to 1.55 Tesla. There are hardly any points on the graph where the value exceeds 2 Tesla. As we move towards the rotor section, the outer edges are depicted in green with a value of approximately 1.16 Tesla. As we approach the shaft, the color changes to blue, and values around 0.25 Tesla are observed. This distribution and pattern make sense for a PMSM motor. The stator region exhibits a higher magnetic field intensity, while the intensity decreases in the rotor region. This reflects the magnetic interaction between the stator and rotor, and it aligns with the operating principle of the motor. The values in the graph depict how the magnetic flux is distributed and where it concentrates.

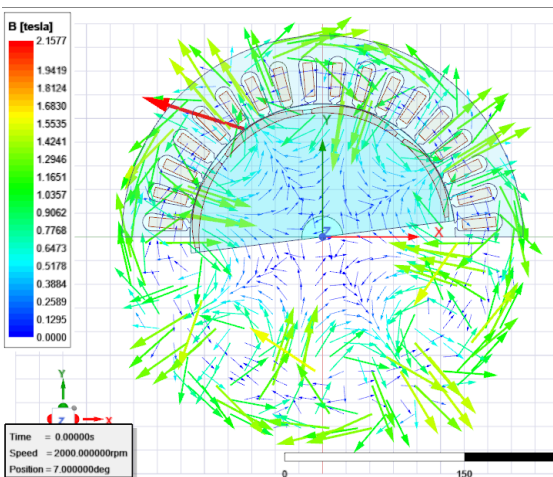


Figure 12. Magnetic Vector Fields Graph

Figure 12 illustrates the vector field of the magnetic flux density. It is worth noting that the magnetic material utilized in the motor does not surpass the saturation point of 2 Tesla. As a result, the motor operates within safe parameters, avoiding any risks of overheating or saturation.

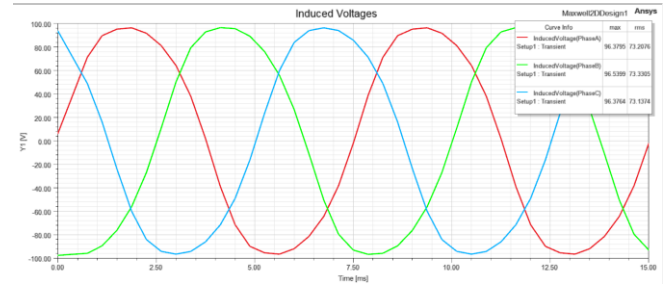


Fig. 13. 2000 rpm 100% load Induced Voltage graph

Figure 13 displays the induced voltage of the motor, which is reported as 96.37 V for phase A. However, it is important to note that this value aligns with the project specifications.

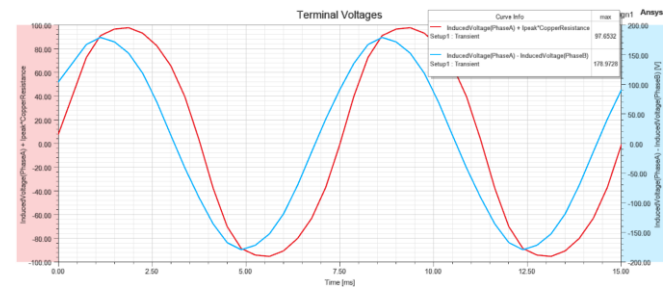


Fig. 14. 2000 rpm 100% load terminal and phase to phase voltages graph

When the terminal voltage value is observed, it is seen that it does not exceed the 100V peak limit. Furthermore, as seen in figure 14, phase-to-phase voltage expresses the difference voltage obtained by subtracting the voltage value of one phase from the voltage value of the other phase. This voltage is generally used in three-phase systems and indicates the potential difference between phases.

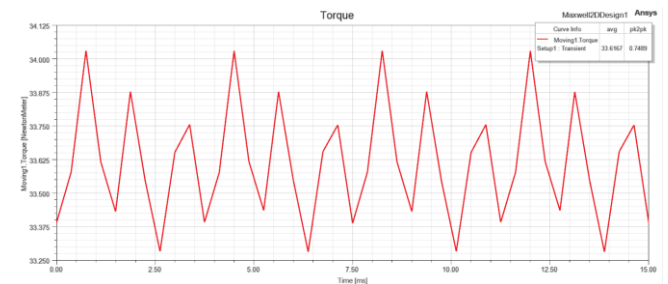


Figure 15. 2000 rpm 100% load torque graph

As can be seen in figure 15, the torque value has reached 33.6167 Nm. This value is sufficient to produce a 7kw motor. In addition, the pick-to-pick value of the torque of the motor is also quite small. When we look at the torque fluctuation of this motor, which has a small value of 0.7489 for the pick-to-pick value, it is observed that it is only 7%.

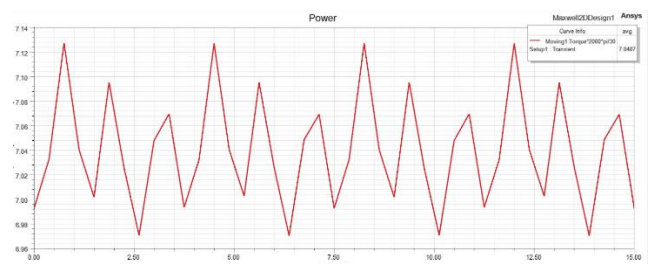


Figure 16. 2000 rpm 100% load output power graph

In addition, the results for 2000 rpm and 50% Load among sixteen different situations seen in the figure 8 are shown graphically below.

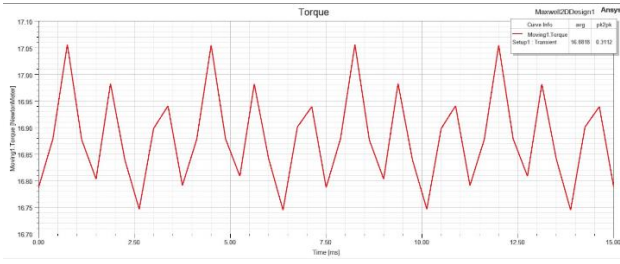


Figure 17. 2000 rpm 50% load torque graph

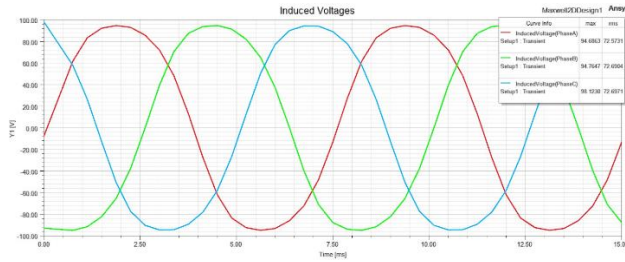


Figure 18. 2000 rpm 50% load Induced Voltage graph

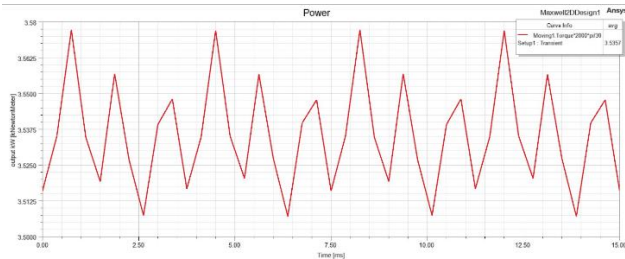


Figure 19. 2000 rpm 50% load Output Power graph

TABLE V. FINAL OUTPUT RESULTS

Output Results	Final Value
Output Power	7.040655 (kW)
Torque Ripple	2.227776 (Nm)
Efficiency	98.76 %
Steel Mass	19.07 (kg)
Magnet Mass	0.25 (kg)
Total Mass	19.32 (kg)
Phase Winding Length	25.573166 (m)
Copper Resistance	0.027689 (Ω)
Copper Area	0.000016 (m^2)
Copper Loss	87.884819 (W)

The output results of the final optimized design are presented in Table V, these results serve as the goal for the values mentioned throughout the rest of the article. The optimized design is visually represented in Figure 9, illustrating the visualization of the motor's enhanced configuration.

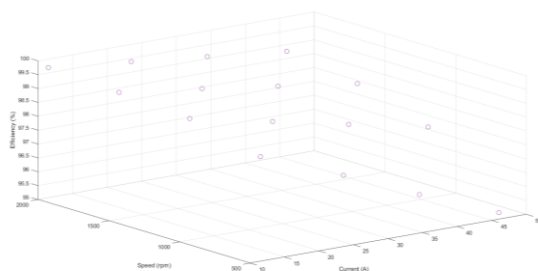


Figure 20. Efficiency, Speed (rpm) and Load results in 3D graph

The graphic you see in Figure 20 represents the efficiency according to current and speed for a total of 16 different conditions. As can be seen from the results, the top left value represents the highest efficiency.

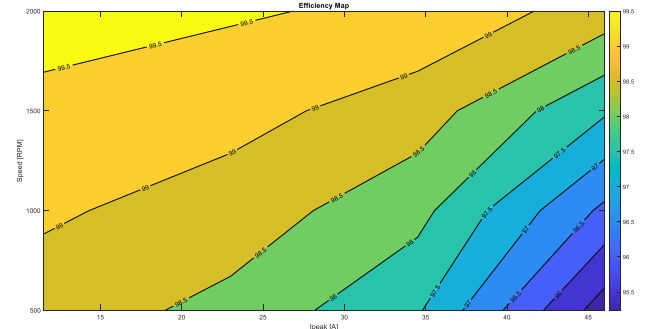


Figure 21. Efficiency Map

The Efficiency Map, depicted in Figure 21, illustrates the efficiency of the PMSM motor across various load conditions. The map utilizes different colors to represent the efficiency levels. Upon observing the figure 21, it is evident that the motor achieves its highest efficiency, transitioning from the blue color to the yellow color.

The project specifications closely align with the results presented in the Results section. However, there may be slight variations between the achieved outputs and the defined objectives, such as a 1V difference in input voltage, 0.05 Nm difference in torque, and a 3-4W difference in power output. These variations can be attributed to factors such as the range of optimization parameters, the prioritization of objectives, and the number of iterations applied during the optimization process.

VII. CONCLUSION

This research study focuses on the design, optimization, and analysis of a permanent magnet synchronous machine (PMSM). The PMSM specifications include 8 poles, 36 slot, a rated power of 7000W, a speed of 2000rpm, a peak voltage of 100V, and a peak current of 46A. The main objective of this research is to develop a cost-effective and efficient PMSM through the application of various optimization techniques. The optimization process aims to minimize losses and ensure that all parameters meet the desired criteria. The ANSYS Electromagnetics Software is utilized for conducting the optimization procedures. As a result, a cost-effective PMSM design is successfully achieved and optimized in accordance with the specified requirements. Additionally, upon analyzing the efficiency graph, it is evident that the highest level of efficiency, reaching 99.69%, is achieved at a 25 percent load and a speed of 2000 rpm.

VIII. REFERENCES

- [1] Agarwal, T. (2019) *Synchronous motor: Working Principle, types, and applications*, *ElProCus*. Available at: <https://www.elprocus.com/synchronous-motor-working-principle-types/> (Accessed: 14 June 2023).
- [2] Hanejko, F. (2020) *Permanent magnet vs induction motor: Torque, losses, material*, *Permanent Magnet vs Induction Motor: Torque, Losses, Material*. Available at: <https://www.horizontechnology.biz/blog/induction-vs-permanent-magnet-motor-efficiency-auto->

electrification#:~:text=Because%20the%20magnets%20are%20permanently,higher%20than%20an%20induction%20motor.

- [3] Liu, X., Lin, Q. and Fu, W. (2017) 'Optimal design of permanent magnet arrangement in synchronous motors', *Energies*, 10(11), p. 1700. doi:10.3390/en10111700.
- [4] Li, X. et al. (2023) 'Design of permanent magnet-assisted synchronous reluctance motor with low torque ripple', *World Electric Vehicle Journal*, 14(4), p. 82. doi:10.3390/wevj14040082.
- [5] Than, A. A., & Ya, A. Z. (2011) 'Design and Analysis of Permanent Magnet Synchronous Motor used in Industrial Robot.' *The Fourth National Conference on Science and Engineering*.
- [6] Tabrizi, M.A. and Radman, G. (2013) 'Detailed dynamic modeling of permanent magnet synchronous machine-based wind turbine for power system dynamic analysis', 2013 *Proceedings of IEEE Southeastcon*. doi:10.1109/secon.2013.6567461.
- [7] Dalcali, a. (2018). Optimal design of high performance interior pm motor for electric vehicle. *The International Journal of Energy and Engineering Sciences*, 3(2), 46-54